Optimisation of the chemical oxidation reduction process (CORD) on surrogate stainless steel in regards to its efficiency and secondary wastes

Aditya Rivonkar, Richárd Katona, Mathurin Robin, Tomo Suzuki-Muresan, Abdessalam Abdelouas, Marcel Mokili, Gergő Bátor, Tibor Kovács

frontiers | Frontiers in Nuclear Engineering

TYPE Original Research
PUBLISHED 02 December 2022
DOI 10.3389/fnuen.2022.1080954

OPEN ACCESS

EDITED BY
Eros Mossini,
Politecnico di Milano, Italy

REVIEWED BY
Vladimir Petrov,
Lomonosov Moscow State University, Russia
Martin Straka,
Nuclear Research Institute Rez, Czechia

*CORRESPONDENCE
Aditya Rivonkar,
rivonkar@subatech.in2p3.fr

SPECIALTY SECTION
This article was submitted to Radioactive Waste Management, a section of the journal Frontiers in Nuclear Engineering

RECEIVED 26 October 2022
ACCEPTED 18 November 2022
PUBLISHED 02 December 2022

CITATION
Rivonkar A, Katona R, Robin M, Suzuki-Muresan T, Abdelouas A, Mokili M, Bátor G and Kovács T (2022), Optimisation of the chemical oxidation reduction process (CORD) on surrogate stainless steel in regards to its efficiency and secondary wastes.
Front. Nucl. Eng. 1:1080954.
doi: 10.3389/fnuen.2022.1080954

Optimisation of the chemical oxidation reduction process (CORD) on surrogate stainless steel in regards to its efficiency and secondary wastes

Aditya Rivonkar[1]*, Richárd Katona[2,3], Mathurin Robin[1], Tomo Suzuki-Muresan[1], Abdessalam Abdelouas[1], Marcel Mokili[1], Gergő Bátor[2,3] and Tibor Kovács[2,3]

[1]Subatech Laboratory, IMT Atlantique CNRS/IN2P3 Nantes University, Nantes, France, [2]Department of Radiochemistry and Radioecology, University of Pannonia, Veszprém, Hungary, [3]Social Organization for Radioecological Cleanliness, Veszprém, Hungary

Nuclear Power is a decarbonated technology of electrical energy generation. Using nuclear energy as a power source is currently considered as the best option in the fight against climate change. But the radioactive waste generated from nuclear power plants and their related facilities are matter of concern. Though the high level and intermediate level activity wastes are contained in small volumes (≤10%), significant volumes of lower activity wastes are generated. Metallic wastes are a major component of these radioactive wastes with about 500,000 tons expected in France alone, including 130,000 tons from steam generators. Majority of these metals are made of Stainless steel 316 alloy or Inconel 600. Under the effect of the primary circuit thermal-hydraulic constraints and irradiation, these the resulting corrosion products may be activated when close to the fuel, and be transported throughout the circuit. These products can be deposited on the surface of other metal components, causing contamination of the latter. The contamination can be adsorbed on the surface but can also diffuse in the oxide layers and sub-surface. The oxide layer is composed of an inner layer of Cr oxide under a layer of Ni and Fe oxide. Chemical decontamination is preferred due to the possibility of decontamination of difficult geometries and tube bends. In order to decontaminate these materials, it is important to dissolve the oxide layers chemically and a few micrometers of base metal where it could have diffused. An existing chemical method used to treat these materials is studied in this article, Chemical Oxidation Reduction Decontamination (CORD). Surrogate steel samples were prepared using high temperature induction heating and water vapour after sample preparation and cleaning. The oxide layer was characterised before treatment of the samples in the batch method at different concentrations and its effects are observed on the dissolution of the oxide layers. A protocol is being developed for the treatment of secondary waste effluents by multi-stage precipitation with a goal to reduce the total waste volumes and thus the volumes of ion exchange resins that would otherwise be needed.

KEYWORDS

radioactive metallic wastes, CORD process, oxide layer, liquid effluent, decontamination technology

1 Introduction

Nuclear power generation is present in many countries worldwide, but more than 60% of the nuclear capacity is over 25 years old. In Europe 90% of all nuclear reactors need to be shut down by 2030, unless their operation life will be prolonged (European Commission, 2016; Volk et al., 2018). The major nuclear decommissioning activity is the application of decontamination technology, which are used to reduce the occupational exposures, to limit the potential releases of radioactive materials and to permit the reuse of components (Murray, 1986; Baja et al., 2009; Hu et al., 2018; Hirose and McCauley, 2022). As a result of decontamination, a wide range and quantity of radioactive waste can be produced, therefore the optimisation of decontamination technologies is a very important issue not only for radiation protection aspects, but in case of radioactive waste management too, to reduce the volumes of secondary wastes generated and/or allow for further processing. (Valencia, 2012; Deng et al., 2020; Shelenkova and Kulagina, 2021). According to the (World Nuclear Waste Report, 2019) 1.4 million m^3 of radioactive wastes will be created by the decommissioning of nuclear facilities in Europe (World Nuclear Waste Report, 2019).

The reactor vessel and the piping system of the primary coolant is typically made up of austenitic stainless steel and Ni-alloy (Airey et al., 1981; Xiong et al., 2022). The alloys are exposed to the corrosion on the internal side under exposure to the primary circuit water, therefore on the surface of these a duplex corrosion layer is formed (Baja et al., 2009; Airey et al., 1981; Varga et al., 2001; Juodis et al., 2019). The upper layer is mainly magnetite and the main part of corrosion film contains Cr, Ni, and Fe mixed oxides (Homonnay et al., 2000; Varga et al., 2002). Generally the thickness of this corrosion layer is 5–6 μm for stainless steel and 2–3 μm for Inconel (Homonnay et al., 2000; Kewther et al., 2001). Under operation the oxide-layer can erode from the surface and can be transported to the high neutron flux reactor core, where the oxides undergo activation (Varga et al., 2001). The activation products circulate throughout the system and deposit on the surface (Padovani, 2020; Chajduk and Bojanowska-Czajka, 2016). The radioactive corrosion products constitute the majority of radioactive contamination (when there is no fuel cladding failure) (Varga et al., 2001).

The Chemical Oxidation Reduction Decontamination (CORD) is a world-wide known 2-steps decontamination process (Radó et al., 2007; Wille et al., 1997). In the first step permanganate ion (MnO_4^-) is used to oxidize the chromium oxide-layer and to release chromate ions (Tian et al., 2019). Permanganate ions are derived from potassium permanganate, which can be used in nitric acid media, which is known as NP CORD or in alkaline media (KOH) which is known as AP CORD.

A third type of the CORD process, HP CORD makes use of permanganic acid which is prepared from $KMnO_4$ using a strong acid cation resin (Demmer, 1994).

In the next step, oxalic acid is added to reduce the permanganate ion to aqueous Mn^{2+} ions and to dissolve the Fe and Ni enriched oxide layer from the surface of the alloys (Tian et al., 2019). The whole process is repeated several times. The solutions are treated with ion exchange resin to extract the dissolved metals, however this process is only used in the second step, because of the incompatibility of the resins with the MnO_2 precipitate that can be formed in the oxidation stage (Campbell et al., 1990). In most cases, the remaining oxalic acid is removed from the solutions by addition of H_2O_2 and the presence of the UV-source (CORD UV technology) (Wille and Bertholdt, 1998). On the basis of technological data the CORD UV process can remove up to 73 kg of corrosion products from a wet surface of 3,300 m^2, while 2900 L of spent resins wastes were generated (Tian et al., 2019). In another study (55 MW—D_2O nuclear reactor) the technology resulted in personnel dose rate savings of 4,500 mSv and produced 1370 L of spent resins (Tian et al., 2019).

In order to reduce the amount of resin used for the treatment of the effluents generated during the CORD process and therefore reduce operating costs, it is possible to precipitate the metals in solution as a first step. Chemical precipitation processes are very effective and well known for reducing radioactive effluent volumes by concentrating radionuclides and metals in solution in solid form (IAEA, 1992; Fu and Wang, 2011; Oncel et al., 2013). One of the authors uses the addition of sodium hydroxide (NaOH) in several steps to precipitate the metals as hydroxides ($M^{(m-n)+}(OH)_n$, where m is charge of the metal) and also to co-precipitate other trace elements by trapping them in the sludge generated. After separating the liquid part from the solid one, the precipitate obtained can be packaged in a suitable matrix and the remaining solution will be treated on ion exchange resins.

It is considered that CORD technology can be performed with high decontamination factors and reasonable efforts, but its optimisation is necessary for economic, technical and further safety reasons (Valencia, 2012; Han et al., 2020). In this study the NP CORD technology efficiency was evaluated on stainless steel decontamination. The efficiency of technologies were analysed in the aspects of the effects of chemicals to the oxide-layer. Further, laboratory tests were carried out to increase the efficiency of the

TABLE 1 Chemical composition of the metal samples (wt%).

Type of metal	C	Si	P	S	Cr	Ni	Ti	Mo	Fe
Stainless Steel 316Ti (1.4571)	≤0.08	≤1	≤0.05	≤0.03	16.5–18.5	10.5–13.5	0.4–0.7	2–2.5	Balance

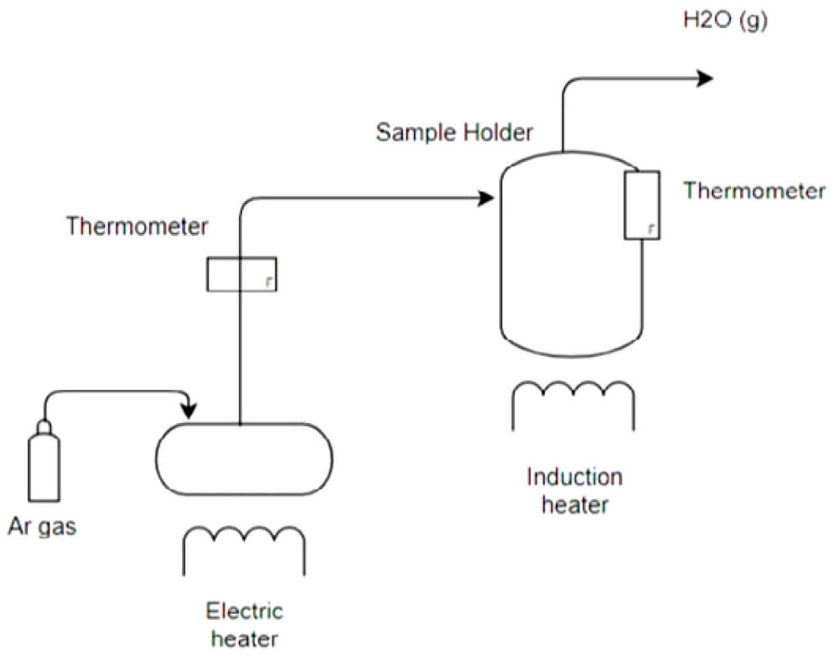

FIGURE 1
Illustration of laboratory set-up to oxidize metal samples [adapted from (Horvath, 2017) and (Katona et al., 2022)].

waste treatment always in accordance with the French waste acceptance criteria.

2 Materials and methods

2.1 Preparation of surrogate steel samples

Non-radioactive, representative metal samples with oxide-layer were used in the testing of NP CORD technology. The composition of the metal samples is presented in Table 1. The samples were 1.5 cm in length, 1.2 cm wide and 0.2 cm thick. The samples were oxidised using the setup shown in Figure 1. The setup used in this work was adapted from D. Horvath (Horvath, 2017) and R. Katona (Katona et al., 2022). The metal samples were inductively heated up to high temperature (600–800°C) and vapours of distilled water/boric acid solutions were passed over it for 8 h. The concentrations of boric acid (ACS reagent, ≥ 99.5%, Merck) solutions were 1 g/L and 15 g/L.

2.2 Treatment of metallic samples using NP CORD and subsequent liquid effluent treatment

2.2.1 Treatment of metallic samples

The dissolution tests were carried out in batch mode wherein the samples were immersed in the solution in glass bottles and placed inside the oven at 80°C for 4 h with stirring at 80RPM for each step of the process. Each sample was placed in silicon polymerized resin (Loctite SI5366, Henkel), and only the oxidised face was exposed to the chemicals. This was done to protect the non-oxidized faces of the metals. The silicon resin was verified to be compatible with the chemicals used. Three different concentrations for potassium permanganate (ACS reagent, ≥99.0%, Merck) were used, 2, 6, and 15 mM in 3 mM nitric acid solution. Likewise, 3 different concentrations for oxalic acid (dihydrate, ACS reagent, ≥95.0%, Alfa Aesar) were used, 5, 10, and 18.5 mM, respectively. Additional oxalic acid was added, for destruction of the potassium permanganate and any MnO_2

formed in solution. For each millimolar of permanganate ion, 1.7 mM of oxalic acid was found to be optimal.

Therefore the final oxalic acid concentrations were a sum of 1.7 times the concentration of potassium permanganate and the additional oxalic acid needed for the dissolution of the oxide film. The final total concentration therefore were, 8.7, 20.8, and 44.0 mM respectively for 2, 6, and 15 mM potassium permanganate.

In order to try to identify a limiting chemical, if any, further tests were carried out with a fixed potassium permanganate concentration (the highest concentration of 15 mM) and varying the oxalic acid concentration as before. Similarly, the potassium permanganate concentration was varied as before and the oxalic acid concentration was fixed (the highest concentration of 18.5 mM).

2.2.2 Secondary liquid treatment

In order to deal with the liquid waste generated during the CORD process, a hydroxide precipitation protocol was optimised by geochemical modelling before being tested on synthetic samples.

2.2.2.1 Modelling

Metal hydroxides have small and very specific precipitation pH ranges, it is necessary to know their solubility constants in order to establish the optimum precipitation pH for each element in solution. The modelling of these constants was carried out on the PhreeqC software (D.L. Parkhurst and C.A.J. Appelo, version 2.18.00). The database used to perform these calculations was created by supplementing the data already in the software (iso, Ilnl, minteq, phreeqc, pitzer, sit) with data from other sources (Gamsjäger et al., 2005; Lemire et al., 2013; Lemire et al., 2020; BRGM Institute, 2020). Modelling was carried out for six different metals (Mn, Ni, Co, Zn, Fe, and Cr) that are part of the contamination present in the primary circuit of a nuclear plant (Pick, 1989; Nuclear Energy Agency, 2014). These metals can come from the composition of the steam generator tubes (mainly Fe, Ni and Cr) but are also activation products present in the primary circuit water (^{51}Cr, ^{54}Mn, ^{55}Fe, ^{58}Co, ^{59}Ni, ^{60}Co, ^{63}Ni, ^{65}Zn) (Hoenes et al., 1980; Walberg et al., 2008). Each metal was analysed independently to establish the optimum pH for precipitation of the hydroxide form. A speciation was also carried out in order to know the different chemical species that could be formed during the experiment. The calculations were carried out for an initial solution (NaCl 0.01 M/25°C) at pH 5 and then in increments of 0.5 until a pH of 14 was reached.

2.2.2.2 Precipitation protocol

To test this protocol, initial tests were carried out on a synthetic sample from metal salts dissolved in 200 ml of water acidified with HNO_3 (70%, Fischer) to reach an initial pH of 2. Five different salts were used to generate the sample: 830 mg/L of manganese dichloride (dihydrate, 99%, Merck); 750 mg/L of nickel nitrate (hexahydrate, 99%, Merck); 120 mg/L of chromium (III) nitrate (nonahydrate, 99%, Acros Organics); 120 mg/L of iron (III) chloride (hexahydrate, 98–102%, Sigma Aldrich) and 10 mg/L of cobalt (II) chloride (hexahydrate, 98%, Sigma Aldrich). For zinc, 2.5 mg/L is added using a standard solution for ICP-MS analysis (1,000 µg/ml, 99.99+%, SCP Science).

After dissolution of the salts, sodium hydroxide 1 M (Titrisol, Merck) is added with constant stirring until a pH of 8.5 using a titration device (716 DMS titrino, Metrohm) and the pH was tracked using a pH meter (Solitrode Pt1000, Metrohm). Stirring is maintained for 2 h before centrifugation (4,000 rpm, 2647G, 15 min). The supernatant is filtered under vacuum (0.2 µm, cellulose acetate, Sartorius Biotech) to remove the last suspended particles and the solid generated is dried in an oven at 50°C for 3 days. A second addition of NaOH 1 M under constant stirring is made to the filtered solution until a pH of 12 is obtained. As in the first precipitation, the solution is first centrifuged and then filtered. The solid produced is also dried in an oven at 50°C for 3 days.

In order to follow the evolution of the concentration of each metal during the purification protocol, 5 ml of solution are taken initially, after the first precipitation and in the final solution. The analysis of these aliquots is then performed by inductively coupled plasma mass spectrometry (ICP-MS).

2.3 Solid Characterisation

The oxide-layers were characterised by Scanning Electron Microscope with Energy Dispersive Spectroscopy (SEM-EDS) and X-ray diffraction (XRD).

D8 Advance, Bruker XRD and Zeiss Merlin SEM devices were used to characterise the formed oxide-layer. XRD measurements were recorded under the following conditions: 10°–100°2theta, a step size of 0.01°, and a scan speed of 4.5 sec/step. SEM analyses of samples were performed by placing them in a phenolic hot mounting resin with carbon filler (Polyfast, Struers). Samples were progressively polished to a 1 µm finish using diamond paste (ADS polycrystaline 1 µm diamond solution, Presi). For imaging, a EHT of 20 kV was used at 400 pA. For EDX analysis, a working distance of 8 mm was used and analysis was carried out at every 1 µm corresponding to the device resolution.

2.4 Liquid characterisation

The efficiency of the chemicals were determined by the measurement of the amount of dissolved metals using Inductively coupled plasma mass spectrometry (X-Series II, Thermo Electron) and electrochemical tests.

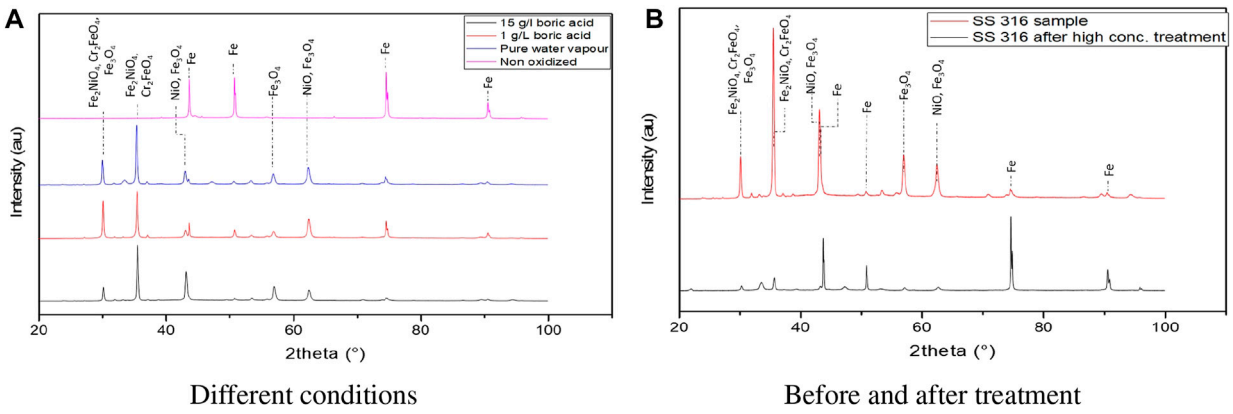

FIGURE 2
XRD profiles the oxidized surrogate steel samples **(A)** Oxidized under different chemical conditions **(B)** Treatment with CORD process at 15 mM $KMnO_4$ and 18 mM oxalic acid (3 cycles); sample oxidized with 15 g/L boric acid.

Tafel-analyses were used to measure the rates of CORD decontamination at various concentrations. Voltalab PGZ201 potentiostat, Radelkis OP-0830P saturated calomel reference electrode (SCE) and stainless steel as a counter electrode were used in these tests. The working electrodes were SS 316Ti stainless steel discs with a diameter of 1.5 cm, which were ground by emery papers down to 180 grit. The polarisation range was ±200 mV with 1 mV/s sweep rate. The equation of the polarisation curve (Butler–Volmer equation) is as follows

$$i = i_0\left(e^{\frac{\beta z_a k}{RT}\Delta E} - e^{\frac{-\alpha z_k F}{RT}\Delta E}\right) \quad (1)$$

In Eq. 1 i is the current density (μA/cm^2), i_0 is the equilibrium current density (μA/cm^2), α/β are the factor of oxidation/reduction, z_a/z_k are the number of the change of the charge numbers and ΔE is the polarisation (V) (Li et al., 2018). The potentials and the equilibrium current densities were determined by Tafel extrapolation. Before the tests the open circuit potential (OCP) was measured for 5 min.

3 Results and discussion

3.1 Characterisation of surrogate steel samples

The XRD characterisation results are presented in Figure 2. The XRD profile of the surrogate samples showed the presence of various oxides of Ni, Fe and Cr such as Fe_3O_4, Fe_2O_3, NiO, Cr_2FeO_4 as seen in Figure 2A. The presence of boric acid appeared to have a small effect on the intensity of the peaks of the various oxides. From Figure 2B, the decrease in intensity of the oxide peaks is observed and the high intensity peaks are arising from base metal, showing effectiveness of the process in removal of the oxide layers.

The SEM images and EDX profiles for a representative sample (sample 3 in Table 2) are seen in Figure 3. Figure 3A shows a magnified image of a treated sample showing both the oxide layer and exposed bare metal. The red line splits the sample, one-half which was exposed to chemicals and the other half, protected by the silicon polymerised resin. An average oxide thickness of 5.0 ± 0.2 μm was seen. The EDX profile of this oxide is seen in Figure 3B. A multi-layered oxide thickness could therefore be seen on this oxide, with the inner layer having an enrichment in Cr and Ni oxide where the outer oxide layer was highly enriched in Fe oxides. These results were found to be coherent to the results obtained by J. Panter (Panter et al., 2006), A. Machet (Machet, 2004), and J. McGrady (McGrady, 2017) who also obtained a multilayer oxide layer, though under contact with high temperature water. Samples 1 and 3 from Table 2, which were oxidized in presence of boric acid, show a decrease in oxide thickness as compared to sample 2, as the concentration of boric acid is increased. This was also observed by Salih et al. (2014); Zhang et al. (2018).

Upon treatment, a disappearance of the majority of the oxide layer is seen in Figure 3C, with small remnants of the inner Cr oxide layer showing effectiveness of the treatment process. The presence of oxide can be attributed to the contribution of the resin.

3.2 Laboratory tests for optimisation of CORD technology

Figure 4 shows the results of the treatment of the samples under different combinations using the CORD process. The results represent the sum of total concentrations of Cr, Fe and

TABLE 2 Summary of effects of boric acid on oxide layers and treatment conditions for different samples.

Sample	Boric acid conc. (g/L)	Oxide thickness (μm)	Dissolution conditions (mM)		Cycles (until total dissolution of oxide)
			$KMnO_4$	Oxalic acid	
1	1	7.40 ± 0.90	2.0	5.3	6
2	0	7.44 ± 1.43	6.3	10.0	6
3	15	5.00 ± 0.20	15.0	18.5	3
4	1	7.40 ± 0.90	15.0	10.0	3
5[a]	0	5.87 ± 0.65	15.0	5.3	3[b]
6[a]	0	6.00 ± 1.29	6.3	18.5	3[b]
7[a]	0	5.77 ± 1.28	2.0	18.5	3[b]

[a]Samples 5,6, and 7 were oxidized in one batch whereas 1–4 were oxidized in a different batch.
[b]Surface was not 100% clean after 3 cycles suggesting need for at least one more cycle.

Ni after 3 cycles of the CORD process. Figure 4A represents the 3 different combinations of concentrations of permanganate and oxalic acid. Samples 1, 2 and 3 from Table 2 were utilised for these tests.The effects of higher efficiency at higher concentrations are evident with the total dissolved metals generally increasing with increase in concentrations across both potassium permanganate and oxalic acid. The selectiveness of the potassium permanganate towards Cr dissolution is also evident with significant higher Cr contents detected after the permanganate step of the process as compared to Fe and Ni. On the other hand, oxalic acid shows a much higher efficiency in dissolution of Fe and Ni whereas no increase in Cr dissolution was noticed across the 3 samples after the oxalic acid step in the process. This confirms the need for an oxidative step in the CORD process for the removal of Cr oxides as found in the literature and a reductive step with oxalic acid for the Fe and Ni oxides (Ocken, 1999; Balaji et al., 2018; Wille and Bertholdt, 1998). The first two concentration combinations required up to 6 cycles for complete removal of the visual oxide layer, though the sample was more or less clean after 5 cycles. Whereas for the combination with the highest concentration required only 3 cycles for complete removal of the visual oxide layer. A summary of the number of cycles applied to various samples is presented in Table 2.

Figure 4B shows the effects of a fixed (high) concentration of oxalic acid with the potassium permanganate concentrations varying as before. Samples 3, 6, and 7 from Table 2 were used for these tests. The higher oxalic acid concentration appeared to affect the number of cycles required, as seen in Table 2 with the surface appearing much cleaner after 3 cycles, as seen in Figure 5A than at lower oxalic acid concentration in Figure 5B.

Similarly, Figure 4C shows the effects of a fixed (high) concentration of potassium permanganate and varying oxalic acid. Samples 3, 4, and 5 from Table 2 were used for these tests. The results here showed less promise at lower oxalic acid concentrations for total dissolution of the oxide layer mainly due to the lower efficiency in dissolution of Fe which is the major component of the oxide layer in stainless steels. The samples did appear to be visually cleaner than those at low concentrations of potassium permanganate as in the case of Figure 4A but this could be due to the smaller size of the oxide layers as seen in Table 2. The results obtained here suggest significant contribution of oxalic acid concentration to the dissolution of the oxide layer for stainless steel arising from its efficacy in dissolution of Fe oxides. Higher overall dissolution of the oxide is observed at higher dissolutions of Fe oxide.

The results presented here do not make use of any UV technology for the oxalic acid stage as suggested by Wille and Bertholdt, (1998) and Ocken, (1999). The results depict the CORD process is effective at all tested concentrations with fewer cycles required at higher concentrations of the acids. This also means higher concentrations of metals found in solution leading to easier precipitation discussed further in Section 3.4. This could suggest the application of the CORD process at a higher concentration without use of UV is possible.

3.3 Electrochemical tests of CORD technology

The polarisation curves of stainless steel 316Ti in 3 mmol/L HNO_3 and 2, 6, 15 mmol/L $KMnO_4$ are presented in Figure 6A. The results of the Tafel-extrapolation are summarised in Table 3.

In Figure 6A the passivisation effects of the strong oxidising agents can be observed. The current densities in the cathodic polarisation curves were higher, when the concentrations of the $KMnO_4$ were increased and the amount of the current in the anodic polarisation decreased by larger $KMnO_4$ concentrations. Further, the anodic polarisation curves showed passive regions. Similar characteristics of polarisation curves were observed with previous studies (Tian et al., 2019). According to the results of

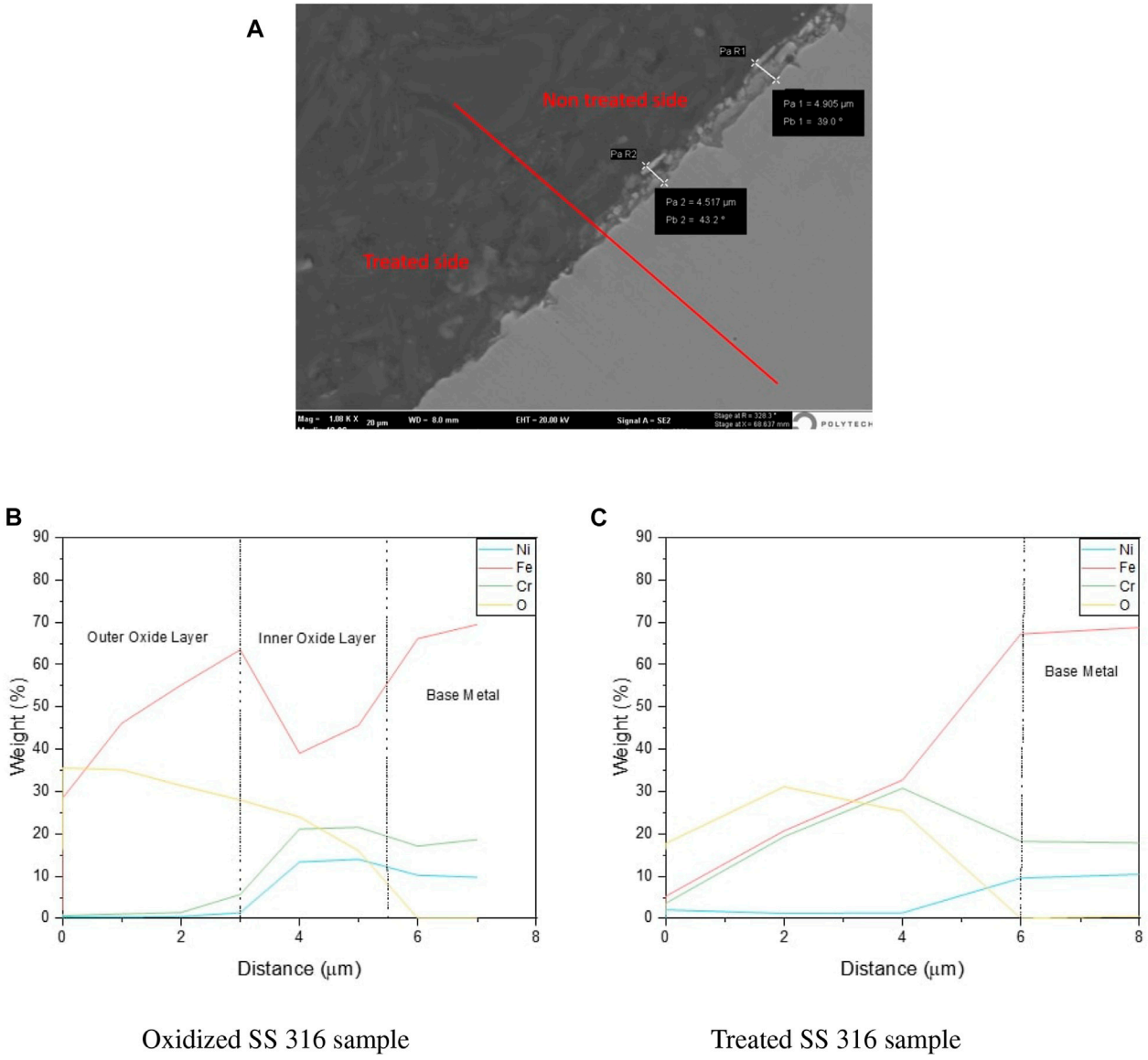

FIGURE 3
SEM characterisation of the SS sample **(A)** Microscope image showing the oxide film and thickness **(B)** EDX profile of the oxide film oxidized in 15 g/L boric acid **(C)** EDX profile after treatment using 15 mM $KMnO_4$ and 18 mM oxalic acid (3 cycles).

Tafel-extrapolation, passivation effects of $KMnO_4$ were significantly higher above 6 mM concentration. The equilibrium current density in 15 mM concentration was more than 4 times higher than in 6 mM and more than 5 times than in 2 mM.

The dissolutions of the oxide-layer from stainless steel samples after treatment with oxalic acid can be seen in Figure 6B. Table 3 shows the results of Tafel-extrapolations. In this case the equilibrium current density continuously increased by dosage of the acid and it reached the maximum at the highest concentration (18.5 mM).

3.4 Treatment of liquid wastes

The modelling of the solubilities of the different metal hydroxides as function of the pH and metallic concentration in solution is shown in Figure 7.

According to the modelling results, the solubilities of metal hydroxides are highly dependent on the pH of the solution. Indeed, it is not possible to fully precipitate all the metals present for a single pH value. It is therefore necessary to carry out several successive precipitations in order to obtain hydroxide slurries containing every metal. These solubility curves correspond to

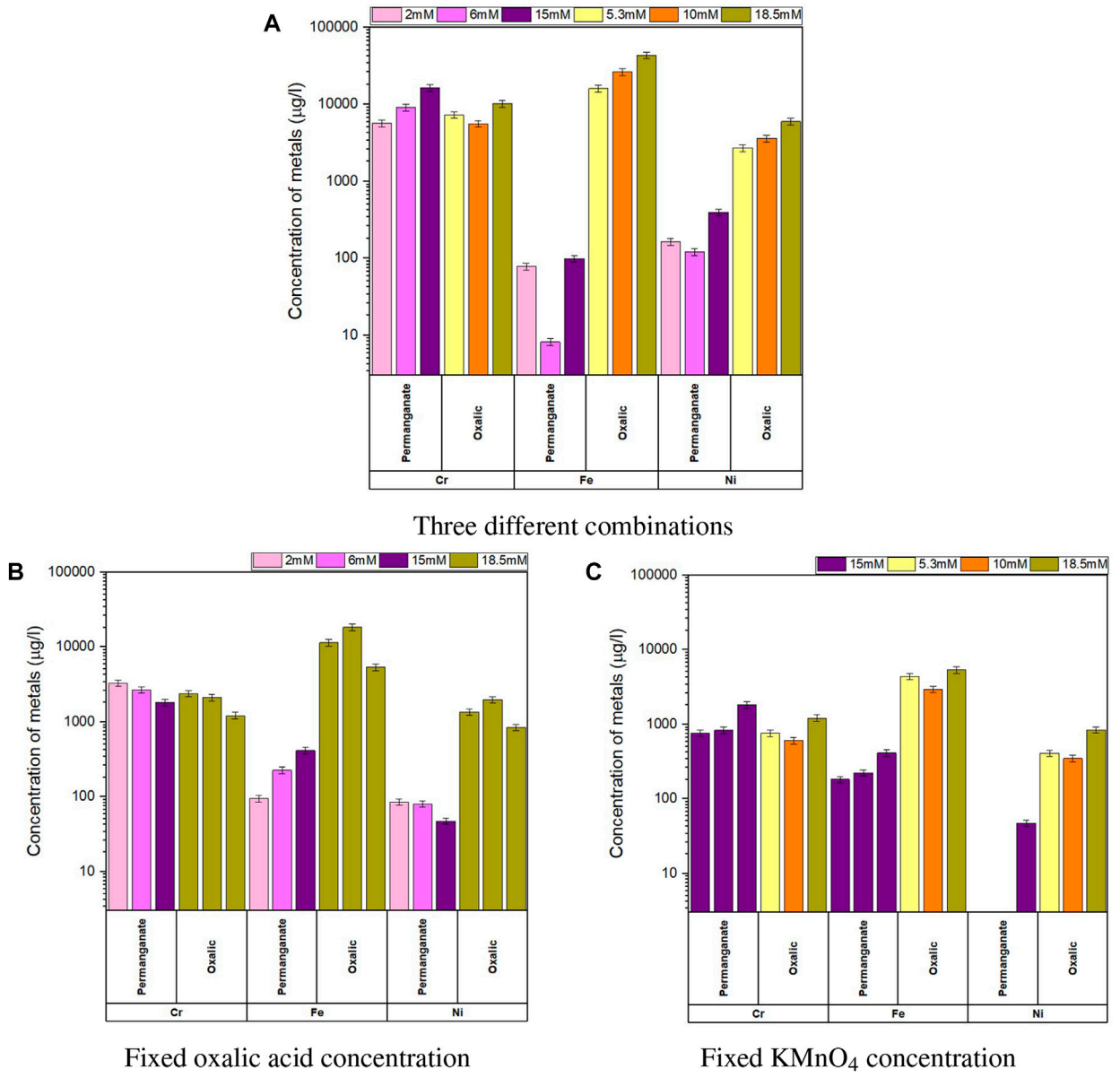

FIGURE 4
ICP-MS results for **(A)** Three conditions of potassium permanganate and oxalic acid concentrations **(B)** Three different potassium permanganate and fixed oxalic acid concentrations **(C)** fixed potassium permanganate and three different oxalic acid concentrations.

those found in the literature (Cravotta, 2008; Oncel et al., 2013). Their model also shows that the pH of 8.5 and 12 are ideal to precipitate the metals of interest. From the solubility curves in Figure 7, it is possible to group the hydroxides according to two precipitation pH values. The first can be carried out at pH 8.5 to precipitate Fe, Cr, and Zn, while the second, at pH 12, removes Mn, Ni and Co. To support this hypothesis, according to an IAEA report, the nuclear research centre of Marcoule in France also adjusts the pH to 8.5 to precipitate iron during the waste treatment (IAEA, 1992).

However, the modelling highlights one of the limitations of the precipitation phenomenon, which is dependent on the concentration of the metals. Indeed, it is not possible to precipitate 100% of the metals in solution because of the solubility limit of the generated hydroxides.

Figure 8 shows the results of the precipitation experiments of a synthetic stainless steel solution to which other metals have been added. Metal concentrations were analysed after each step of the test. These data show the importance of carrying out two separate precipitations for two different pH values. Indeed, some

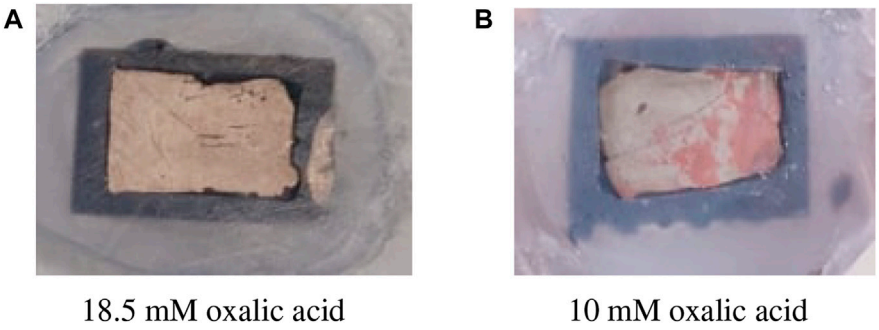

FIGURE 5
Effect of oxalic acid concentration after 3 cycles at 15 mM potassium permanganate **(A)** 18.5 mM oxalic acid **(B)** 10 mM oxalic acid.

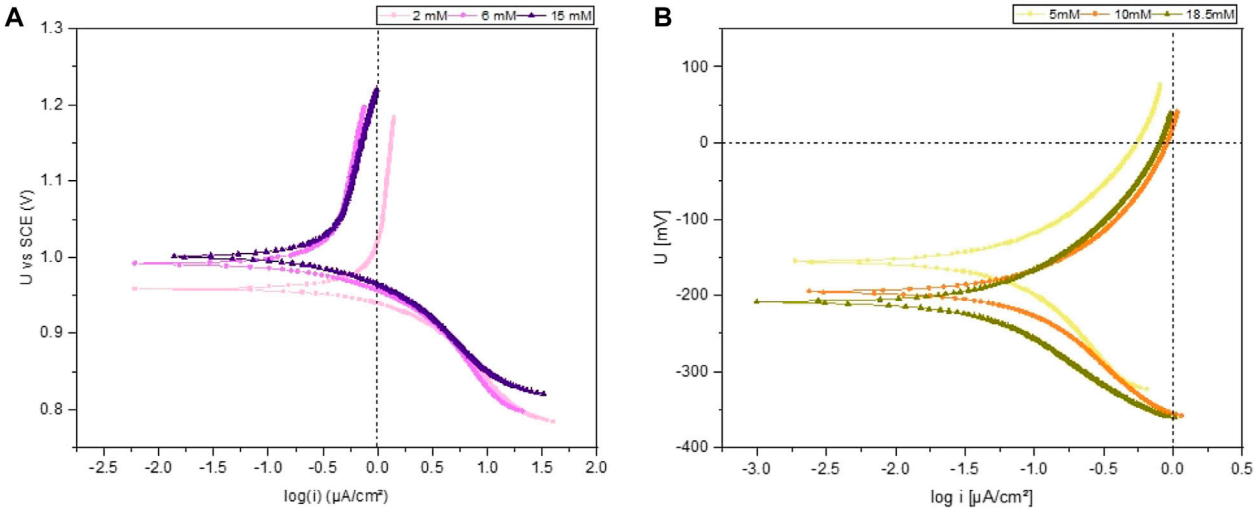

FIGURE 6
Polarisation curves of SS 316Ti in decontamination liquid with **(A)** different $KMnO_4$ concentration in presence of 3 mM nitric acid **(B)** different oxalic acid concentration.

TABLE 3 Equilibrium current densities, equilibrium potential and the Tafel-slopes in decontamination liquids.

	E (i = 0)	i0	α	β
	[V]	[μA/cm^2]	[mV]	[mV]
2 mM $KMnO_4$ + 3 mM HNO_3	0.956	1.965	—	−169
6 mM $KMnO_4$ + 3 mM HNO_3	0.988	1.504	—	−199
15 mM $KMnO_4$ + 3 mM HNO_3	0.998	0.362	515	−104
5 mM oxalic acid	−0.158	0.079	167	−218
10 mM oxalic acid	−0.198	0.085	140	−167
18.5 mM oxalic acid	−0.211	0.163	297	−214

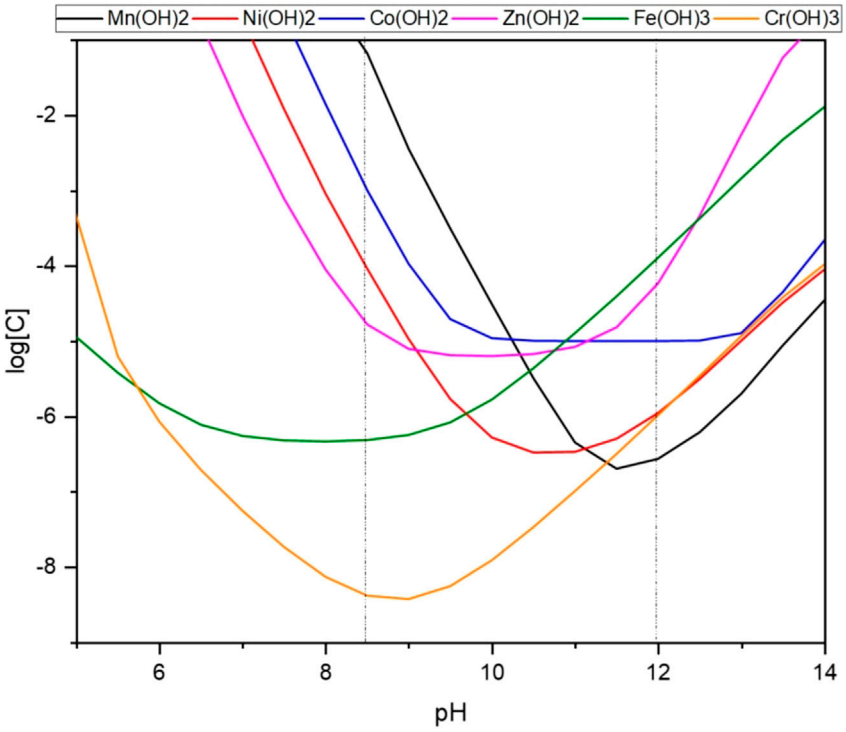

FIGURE 7
Phreeqc modelling the solubility of several metal hydroxides as function of pH.

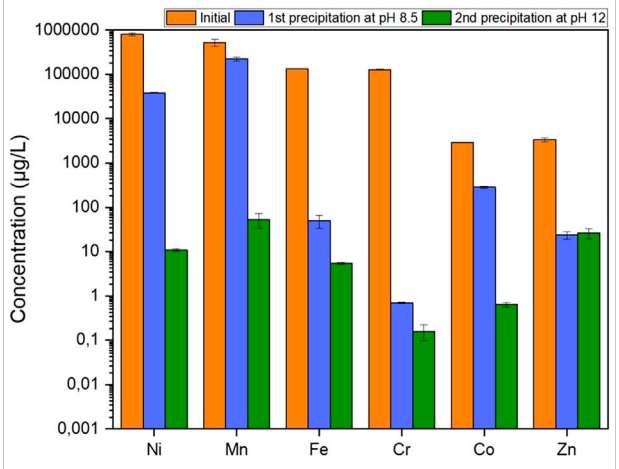

FIGURE 8
Hydroxide precipitation results on a synthetic sample.

metals such as iron, chromium, zinc seem to precipitate mainly at pH 8.5 but others metals like manganese, nickel and cobalt require a second precipitation at pH 12 to be have higher removal efficiency. The first precipitation removes up to 99.99% of Cr, 57.20% of Mn, 99.96% of Fe, 90.21% of Co, 95.23% of Ni and 99.30% of Zn. This also corresponds to the removal efficiency observed by Oncel et al. (2013) who found 99.96% for Fe, 99.50% for Cr and 99.59% for Zn for a precipitation at pH 8, therefore portraying the reliability of the method. After the second precipitation, a total of 99.99% of Cr, Mn, Fe, Zn and 99.98% of Co, and 99.23% of Ni have been removed. During this step, manganese is almost totally removed from the solution compared to the first precipitation at pH 8.5. This behaviour was also observed by Balintova and Petrilakova (2011) where 16% of the manganese was removed at pH 8.2 and 89.49% at pH 9.98. The results are also coherent with those obtained from modelling the solubility of hydroxides in Figure 7.

Some fission products like Sr, Cs, Pu, Am, and Ce, could also be found in solution. These elements were not modelled because of their very low concentrations compared to the ones selected in Figure 7. According to Lehto and Hou (2010), Am precipitates as $Am(OH)_3$ between pH 11 and 12, Pu is expected to precipitate as $Pu(OH)_4$ for a pH $>$ 6 as concurred by Stroud et al. (2006). For Ce, it precipitates as $Ce(OH)_3$ from pH 8.5 according to Bouchaud et al. (2012). Whereas for Sr, 99% of the hydroxide complex $Sr(OH)_2$ remains in solution at pH $\approx$ 13 and in the pH range (6–12) targeted in this work, Cs remains in solution as Cs^+ as seen by Bull (1974). The removal of these soluble fission

products such as Cs and Sr along with other traces would require extraction using ion exchange resins.

The results in Figure 8 were obtained from a synthetic sample generated with dissolved metal salts. At the end, the final concentrations obtained at the end of the protocol are between 0.05 and 60 μg/L for initial concentrations between 1 and 800 mg/L. Based on the information of AmberLite IRN97 H Ion Exchange Resin (Dupont Water Solutions), which is a potential nuclear grade strong acid cation resin used in extracting of the dissolved metals, calculations were done to simulate the amount of resin saved by using the precipitation protocol. According to the total exchange capacity of the resin (≥2.1 eq/L), the initial volume of the solution (250 ml) and the concentrations of metals in Figure 8 and an assumed efficiency of 20%, a theoretical estimate of 30 g of resin would be required without the precipitation protocol as opposed to just 2.5 mg with. This represents a reduction of 99.99% in the amount of resin required. The estimate here doesn't account for the added Na^+ content in solution nor the K^+ in solution and only estimates the requirements for the dissolved metals. Additional volumes of the resin would therefore be required to retain the K^+ and Na^+ from the solution. Further tests are required for the precipitation protocol using KOH instead of NaOH, which could avoid the addition of Na^+ into the solution at the cost of increased K^+ concentration. The resin, Amberlite IRN97 H can also be used in the removal of K^+ (Dupont Water Solutions, 2019).

The combined mass of the sludge across the two precipitation steps on the synthetic sample in Figure 8 was approximately 14.5 g. Upon drying, the total precipitate weighed approximately 0.7 g, suggesting about 95% of weight is lost in water during drying. Cements and geopolymers are potential candidates for the final conditioning of these precipitates but these require evaluation in terms of mechanical resistance, and radio-chemical resistance and durability.

However, the CORD process uses oxalic acid, which is found in the liquid waste. It is known that some metals can form a complex $M(C_2O_4)$ which can be soluble in solution like chromium oxalate, which was also seen in a literature study (Remoundaki et al., 2007). Preliminary tests were carried out on the surrogate metal samples without destruction of oxalic acid, and the initial results portrayed lower precipitation levels mainly arising from Cr. This data and the pictures of the solution at different pH can be found in the supplementary data in Supplementary Figures S2, S3, and S4. Therefore, it is necessary to destroy the remaining oxalic acid before the precipitation process. Preliminary tests have shown the use of H_2O_2 under heating is a viable option to destroy oxalic acid, and the results can be found in supplementary data in Supplementary Figure S5.

4 Conclusion

In this study, the two-step CORD technology was analysed with respect to the radioactive waste management while keeping in mind the waste acceptance criteria. Non-radioactive, representative surrogate metal samples were prepared in the laboratory and the effects of the chemical treatments were studied on these surrogate samples. After the characterisation of the oxide layers, the efficiency of the chemical treatment was determined by the measurements of the dissolved metal ions and the efficiency confirmed by the electrochemical tests. Laboratory tests were also carried out to decrease the volume of the final effluents by means of precipitation.

On the surface of surrogate samples, and approximately 6 μm thick multi-layered corrosion was developed using the laboratory technique in high temperature water vapour conditions. The oxide-layer thickness reduced, when boric acid was added to the water vapour. In any case, the outer layer of the oxide was enriched in Fe, and the inner layer was enriched in Cr and Ni oxides. The technique of preparation of surrogate samples using high temperature water vapour resulted in the oxide layer being a good representation of the samples based on the characterisation results and the literature review.

The CORD process showed a good capacity in dissolution of the oxide films at all concentrations, from very low to higher concentrations of both potassium permanganate and oxalic acid, depending on the number of cycles used. The potassium permanganate mostly had an affect on the dissolution of Cr whereas oxalic acid concentrations affected the dissolution of Fe and Ni. This was also confirmed by the results of the electrochemical tests. The reduction of $KMnO_4$ was determinant and the corrosion of the metal samples was only detected in the steps of oxalic acid treatments. The efficiency increases as concentration increases, the higher concentration dissolution appears to be more promising in terms of time of treatment and also, a higher concentration in metals in solution at each stage implies a more effective precipitation process for treatment of the effluent waste.

The precipitation protocol for synthetic samples appears to be highly effective with about 83.57% of the metals removed after the first precipitation and 99.99% after the second one. The protocol is fast and cheap and requires only NaOH addition to reach the desired pH. This suggests significantly lower volumes of cation resins being used which leads to lower volumes of final wastes and therefore lower costs.

One major aspect not covered in this article is an intermediate step in between the two stages, treatment of metals and precipitation of the metal ions in the effluents, is the destruction of remaining oxalic acid. A protocol for thermal decomposition of the remaining oxalic acid is being developed. Preliminary results can be found in the supplementary data.

Data availability statement

The original contributions presented in the study are included in the article/Supplementary Material, further inquiries can be directed to the corresponding author.

Author contributions

AR: Methodology, Validation, Formal analysis, Investigation, Visualization, Data Curation, Writing—Original Draft, Writing–Review and Editing RK: Formal analysis, Data curation, Methodology, Resources, Writing—Original Draft. MR: Formal analysis, Data curation, Methodology, Writing—Original Draft, Writing–Review and Editing TS-M: Methodology, Validation, Supervision, Writing–Review and Editing AA: Conceptualization, Supervision, Funding acquisition, Project administration, Writing–Review and Editing MM: Validation, Supervision, Methodology. GB: Conceptualization, Formal analysis, Supervision. TK: Conceptualization, Formal analysis, Supervision.

Funding

This work was carried out under the PREDIS European project. This project has received funding from the European Union's Horizon 2020 research and innovation programme under agreement No 945098.

Acknowledgments

We would like to thank Florence Carette of EDF, for her guidance and support throughout the work. A special thanks also to Jean Rouxel Institute of Materials in Nantes, France (IMN) and to Marion Allart, former employee at IMN, for the training and access to the SEM facilities.

Conflict of interest

The authors declare that the research was conducted in the absence of any commercial or financial relationships that could be construed as a potential conflict of interest.

Publisher's note

All claims expressed in this article are solely those of the authors and do not necessarily represent those of their affiliated organizations, or those of the publisher, the editors and the reviewers. Any product that may be evaluated in this article, or claim that may be made by its manufacturer, is not guaranteed or endorsed by the publisher.

Supplementary material

The Supplementary Material for this article can be found online at: https://www.frontiersin.org/articles/10.3389/fnuen.2022.1080954/full#supplementary-material.

References

Airey, G. P., Vaia, A. R., and Aspden, R. G. (1981). A stress corrosion cracking evaluation of Inconel 690 for steam generator tubing applications. *Nucl. Technol.* 55, 436–448. doi:10.13182/NT55-436

Baja, B., Varga, K., Szabó, N. A., Németh, Z., Kádár, P., Oravetz, D., et al. (2009). Long-term trends in the corrosion state and surface properties of the stainless steel tubes of steam generators decontaminated chemically in VVER-type nuclear reactors. *Corros. Sci.* 51, 2831–2839. doi:10.1016/j.corsci.2009.08.007

Balaji, V., Chandramohan, P., Rangarajan, S., and Velmurugan, S. (2018). Dissolution of nickel and chromium from Ni-Cr-Fe-O oxide by oxidative treatment with permanganate. *Prog. Nucl. Energy* 104, 136–142. doi:10.1016/j.pnucene.2017.09.008

Balintova, M., and Petrilakova, A. (2011). Study of pH influence on selective precipitation of heavy metals from acid mine drainage. *Chem. Eng. Trans.* 25, 345–350. doi:10.3303/CET1125058

Bouchaud, B., Balmain, J., Bonnet, G., and Pedraza, F. (2012). ph-distribution of cerium species in aqueous systems. *J. Rare Earths* 30, 559–562. doi:10.1016/S1002-0721(12)60091-X

BRGM Institute (2020). Thermodynamics. *A Phreeqc database*. Available at: https://thermoddem.brgm.fr/databases/phreeqc (Accessed September 8, 2022)

Bull, P. S. (1974). "Removal of strontium and cesium from radioactive waste waters by coagulation-flocculation of ferric hydroxide," (Kensington, Australia: University of New South Wales). Ph.D. thesis.

Campbell, D., Lee, D., and Dillow, T. (1990). "Ion-exchange processes for low-level liquid waste treatment," in Proceedings of the international meeting on nuclear and hazardous waste management (United States), Oak Ridge National Lab, TN, December 1, 1991, 1. doi:10.2172/6036184

Chajduk, E., and Bojanowska-Czajka, A. (2016). Corrosion mitigation in coolant systems in nuclear power plants. *Prog. Nucl. Energy* 88, 1–9. doi:10.1016/j.pnucene.2015.11.011

Cravotta, C. A. (2008). Dissolved metals and associated constituents in abandoned coal-mine discharges, Pennsylvania, USA. Part 2: Geochemical controls on constituent concentrations. *Appl. Geochem.* 23, 203–226. doi:10.1016/j.apgeochem.2007.10.003

Demmer, R. (1994). *Testing and evaluation of eight decontamination chemicals WINCO–1228*. United States: WestingHouse Idaho Nuclear Company, Inc.

Deng, D., Zhang, L., Dong, M., Samuel, R. E., Ofori-Boadu, A., and Lamssali, M. (2020). Radioactive waste: A review. *Water Environ. Res.* 92, 1818–1825. doi:10.1002/wer.1442

Dupont Water Solutions (2019). *AmberLite IRN97 H ion exchange resin product data sheet*.

European Commission (2016). *Nuclear illustrative programme, ref: Com(2016) 177*. Luxembourg: Official Journal of the European Union, 104–110.

Fu, F., and Wang, Q. (2011). Removal of heavy metal ions from wastewaters: A review. *J. Environ. Manag.* 92, 407–418. doi:10.1016/j.jenvman.2010.11.011

Gamsjäger, H., Bugajski, J., Gajda, T., Lemire, R., and Preis, W. (2005). *Chemical thermodynamics of nickel*. Paris, France: Nuclear Energy Agency.

Han, S., Hong, S., Nam, S., Kim, W.-S., and Um, W. (2020). Decontamination of concrete waste from nuclear power plant decommissioning in South Korea. *Ann. Nucl. Energy* 149, 107795. doi:10.1016/j.anucene.2020.107795

Hirose, R., and McCauley, D. (2022). The risks and impacts of nuclear decommissioning: Stakeholder reflections on the UK nuclear industry. *Energy Policy* 164, 112862. doi:10.1016/j.enpol.2022.112862

Hoenes, G. R., Mueller, M. A., and Mccormack, W. D. (1980). *Radiological assessment of steam generator removal and replacement : Update and revision national technical informati on service*. Washington D.C: Office of Nuclear Reactor Regulation NUREG/CR, 1–52.

Homonnay, Z., Vértes, A., Kuzmann, E., Varga, K., Baradlai, P., Hirschberg, G., et al. (2000). Effects of AP-CITROX decontamination procedure on the surface oxide layer composition of stainless steel originating from the primary circuit of a VVER-type nuclear reactor. *J. Radioanalytical Nucl. Chem.* 246, 131–136. doi:10.1023/a:1006761921604

Horvath, D. (2017). *Development and application of multipurpose radiotracer methods for the investigation of sorption processes on structural material surfaces*. Veszprém: University of Pannonia. Ph.D. thesis. doi:10.18136/PE.2017.665

Hu, Y., Long, X., Dong, L., Tan, Z., Tang, W., and Huang, Z. (2018). A decontamination technique for the primary cooling circuit of the research type nuclear reactor. *Nucl. Eng. Des.* 337, 318–323. doi:10.1016/j.nucengdes.2018.07.019

IAEA (1992). *Chemical precipitation processes for the treatment of aqueous radioactive waste*. Vienna: Intenational Atomic Energy Agency, 337.

Juodis, L., Maceika, E., Plukis, A., Dacquait, F., Genin, J., and Benier, G. (2019). Assessment of radioactive contamination in primary circuit of WWER-440 type reactors by computer code OSCAR for the decommissioning case. *Prog. Nucl. Energy* 110, 191–198. doi:10.1016/j.pnucene.2018.09.019

Katona, R., Rivonkar, A., Locskai, R., Bátor, G., Abdelouas, A., Somlai, J., et al. (2022). Tafel-analysis of the ap-citrox decontamination technology of inconel alloy 690. *Appl. Radiat. Isotopes* 181, 110073. doi:10.1016/j.apradiso.2021.110073

Kewther, A., Hashmi, M. S. J., and Yilbas, B. S. (2001). Corrosion properties of Inconel 617 alloy after heat treatment at elevated temperature. *J. Mat. Eng. Perform.* 10, 108–113. doi:10.1361/105994901770345420

Lehto, J., and Hou, X. (2010). *Chemistry and analysis of radionuclides: Laboratory techniques and methodology*. New Jersey, United States: Wiley.

Lemire, R., Berner, U., Musikas, C., Palmer, D., Taylor, P., and Tochiyama, O. (2013). *Chemical thermodynamics of iron, Part 1*. Paris, France: Nuclear Energy Agency. 13a.

Lemire, R., Palmer, D., Taylor, P., and Schlenz, H. (2020). *Chemical thermodynamics of iron, Part 2*. Paris, France: Nuclear Energy Agency. 13b.

Li, D., Lin, C., Batchelor-McAuley, C., Chen, L., and Compton, R. G. (2018). Tafel analysis in practice. *J. Electroanal. Chem.* 826, 117–124. doi:10.1016/j.jelechem.2018.08.018

Machet, A. (2004). "Study of the initial stages of oxidation of stainless steels in high temperature water," (Paris, France: Chimie ParisTech), 235. Chemical Sciences.

McGrady, J. (2017). "The effect of water Chemistry on corrosion product build-up under PWR primary coolant conditions," (Manchester: University of Manchester). Ph.D. thesis.

Murray, A. (1986). A chemical decontamination process for decontaminating and decommissioning nuclear reactors. *Nucl. Technol.* 74, 324–332. INIS Reference Number: 18022986. doi:10.13182/NT86-A33835

Nuclear Energy Agency (2014). *Radiation protection aspects of primary water chemistry and source-term management report*. Singapore: Radiological Protection NEA/CRPPH/R, 122. 2.

Ocken, H. (1999). *Decontamination handbook*. Palo Alto, CA: EPRI, 112352.

Oncel, M. S., Muhcu, A., Demirbas, E., and Kobya, M. (2013). A comparative study of chemical precipitation and electrocoagulation for treatment of coal acid drainage wastewater. *J. Environ. Chem. Eng.* 1, 989–995. doi:10.1016/j.jece.2013.08.008

Padovani, C. (2020). in *Chap. 9. European federation of corrosion (EFC) series* (Sawston, United Kingdom: Woodhead Publishing), 341–370. doi:10.1016/B978-0-12-823719-9.00009-3. *The corrosion behavior of stainless steel in conditions relevant to the storage of intermediate level radioactive waste*

Panter, J., Viguier, B., Cloué, J.-M., Foucault, M., Combrade, P., and Andrieu, E. (2006). Influence of oxide films on primary water stress corrosion cracking initiation of alloy 600. *J. Nucl. Mater.* 348, 213–221. doi:10.1016/j.jnucmat.2005.10.002

Pick, M. (1989). *Summary of work on characterization of the radioactive deposits on pwr primary circuit surfaces*. Vienna, Austria: IAEA-TECDOC, 79–92. 511. doi:10.1016/0143-148x(81)90034-3

Radó, K., Varga, K., Németh, Z., Varga, I., Somlai, J., Oravetz, D., et al. (2007). A systematic study of the corrosion effects of the framatome CORD-UV technology. *Acad. Appl. Res. Mil. Sci.* 3, 171–175. doi:10.1533/9781845693466.4.316

Remoundaki, E., Hatzikioseyian, A., and Tsezos, M. (2007). A systematic study of chromium solubility in the presence of organic matter: Consequences for the treatment of chromium-containing wastewater. *J. Chem. Technol. Biotechnol.* 82, 802–808. doi:10.1002/jctb.1742

Salih, S., Gad-Allah, A., Abd El-Wahab, A., and Abd El-Rahman, H. (2014). Effect of boric acid on corrosion and electrochemical performance of Pb-0.08{\%} Ca-1.1 {\%} Sn alloys containing Cu, As, and Sb impurities for manufacture of grids of lead-acid batteries. *Turk. J. Chem.* 38, 260–274. doi:10.3906/kim-1212-76

Shelenkova, V., and Kulagina, T. (2021). Refinment of a decontamination technology for radioactively contaminated equipment. *Radioact. Waste* 14, 28–38. doi:10.25283/2587-9707-2021-1-28-38

Stroud, M. A., Salazar, R. R., Abney, K. D., Bluhm, E. A., and Danis, J. A. (2006). Purification of plutonium chloride solutions via precipitation and washing. *Sep. Sci. Technol.* 41, 2031–2046. doi:10.1080/01496390600742997

Tian, Z., Song, L., and Li, X. (2019). Effect of oxidizing decontamination process on corrosion property of 304L stainless steel. *Int. J. Corros.* 2019, 1–6. doi:10.1155/2019/1206098

Valencia, L. (2012). Radioactive waste management in nuclear decommissioning projects. *Nucl. decommissioning Plan. Exec. Int. Exp.* 36, 375–415. doi:10.1533/9780857095336.2.375

Varga, K., Hirschberg, G., Németh, Z., Myburg, G., Schunk, J., and Tilky, P. (2001). Accumulation of radioactive corrosion products on steel surfaces of VVER-type nuclear reactors. II. ^{60}Co. *J. Nucl. Mater.* 298, 231–238. doi:10.1016/S0022-3115(01)00658-4

Varga, K., Németh, Z., Somlai, J., Varga, I., Szánthó, R., Borszéki, J., et al. (2002). Hydrodynamics of the effectiveness of the AP-CITROX decontamination technology. *J. Radioanal. Nucl. Chem.* 254, 589–596. doi:10.1023/A:1021662726609

Volk, R., Hübner, F., Hünlich, T., and Schultmann, F. (2018). The future of nuclear decommissioning – A worldwide market potential study. *Energy Policy* 124, 226–261. doi:10.1016/j.enpol.2018.08.014

Walberg, M., Viermann, J., Beverungen, M., Kemp, L., Lindström, A., Gesellschaft, G. N. S., et al. (2008). "Disposal of steam generators from decommissioning of PWR nuclear power plants," in Iync 2008, Interlaken, Switzerland, 20 – 26 September 2008, 20–26.

Wille, H., and Bertholdt, H. (1998). *Recent developments and experience with the cord uv process*. Japan: Japan Atomic Industrial Forum, Inc.

Wille, H., Bertholdt, H., and Roumiguiere, F. (1997). *Chemical decontamination with the CORD UV process: Principle and field experience*. Slovenia: Nuclear Energy in Central Europe, 199–208.

World Nuclear Waste Report (2019). *The world nuclear waste report. 2019-Focus, Europe*. Berlin, Germany: Heinrich-Böll-Stiftung.

Xiong, Y., Watanabe, Y., Shibayama, Y., Zhong, X., and Mary, N. (2022). Low-cycle fatigue behaviors of 316l austenitic stainless steel in high temperature water: Effects of pre-soaking, dissolved oxygen, and boric acid & lithium hydroxide. *Nucl. Eng. Technol.* 54, 3215–3224. doi:10.1016/j.net.2022.04.003

Zhang, S., Lu, Q., Xu, Y., He, K., Liang, K., and Tan, Y. (2018). Corrosion behaviour of 316L stainless steel in boric acid solutions. *Int. J. Electrochem. Sci.* 13, 3246–3256. doi:10.20964/2018.04.33